Ross Ice Shelf Displacement and Elastic Plate Waves Induced by Whillans Ice Stream Slip Events

Douglas A. Wiens[1], Richard C. Aster[2], Andrew A. Nyblade[3], Peter D. Bromirski[4], Peter Gerstoft[4], Ralph A. Stephen[5]

[1]Department of Earth and Planetary Sciences, Washington University, Saint Louis, MO, USA

[2]Department of Geosciences and Warner College of Natural Resources, Colorado State University, Fort Collins, CO, USA

[3]Department of Geosciences, Pennsylvania State University, University Park, PA, USA

[4]Scripps Institution of Oceanography, University of California San Diego, La Jolla, CA, USA

[5]Woods Hole Oceanographic Institution, Woods Hole, MA, USA

Corresponding author: Douglas Wiens (doug@wustl.edu)

Key Points:

- Extensional Lamb waves propagate across the Ross Ice Shelf, radiated from slip events at the base of the Whillans Ice Stream
- During the passage of the Lamb waves, the entire ice shelf is displaced about 60 mm, with a velocity an order of magnitude above its long-term flow rate.
- The displacement pulses produce a peak dynamic strain of 10^{-7}, suggesting that they could trigger icequakes in the ice shelf.

Abstract

Ice shelves are assumed to flow steadily from their grounding lines to the ice front. We report the detection of ice-propagating extensional Lamb (plate) waves accompanied by pulses of permanent ice shelf displacement observed by co-located GNSS receivers and seismographs on the Ross Ice Shelf. The extensional waves and associated ice shelf displacement are produced by tidally triggered basal slip events of the Whillans Ice Stream, which flows into the ice shelf. The propagation velocity of 2800 m/s is intermediate between shear and compressional ice velocities, with velocity and particle motions consistent with predictions for extensional Lamb waves. During the passage of the Lamb waves the entire ice shelf is displaced about 60 mm with a velocity more than an order of magnitude above its long-term flow rate. Observed displacements indicate a peak dynamic strain of 10^{-7}, comparable to that of earthquake surface waves that trigger ice quakes.

Plain Language Summary

Ice shelves normally flow steadily towards their boundaries with the open ocean at the ice front. However, seismographs and GNSS recievers deployed on the Ross Ice Shelf record guided elastic plate waves traveling in the ice as well as permanent displacement of the ice shelf. The elastic waves and ice shelf displacement originate from basal slip events of the Whillans Ice Stream, which flows into the Ross Ice Shelf. The velocity of the elastic waves is about 2800 m/s, as expected for guided plate waves propagating in an ice shelf. During the passage of the elastic waves, the entire ice shelf with an area of 500,000 square kilometers is displaced about 60 mm in a direction away from the Whillans Ice Stream. These observations show that the strain imparted to the ice shelf by the once or twice daily Whillans Ice Stream basal slip events is sufficient to trigger ice quakes and perhaps enhance the deformation of the ice shelf.

1 Introduction

The interactions between ice streams and ice shelves are highly important for the dynamics and stability of continental ice sheets and shelves. Ice shelves provide restraining forces to their associated ice streams and glaciers which act to resist their motion, commonly referred to as a buttressing effect (Dupont and Alley, 2005; Goldberg et al, 2009). Ice sheet models show that disintegration of ice shelves increases the velocities of the associated ice streams and leads to rapid ice sheet thinning and ice mass loss (Joughlin et al, 2012; Martin et al, 2019). Collapse of ice shelves along the Antarctic Peninsula has resulted in increased motion and thinning of surrounding glaciers (Scambos et al., 2004; Berthier et al., 2012). These observations have brought increasing attention to the stability of ice shelves and to their interactions with upstream ice streams and glaciers.

Ice streams generally move at a relatively constant velocity over low friction basal surfaces from the ice sheet interior to their grounding lines, where they often terminate into ice shelves. Ice shelves similarly move smoothly over the ocean from the grounding lines to the ice shelf calving front. The motion of both ice streams and ice shelves is modulated by tides, but this occurs gradually in association with tidal cycles (Anandakrishnan et al, 2003; Brunt et al., 2010; Klein et al, 2020). The Whillans Ice Stream (WIS) in West Antarctica (Figure 1) represents an exception to this general rule, as it undergoes one or two tidally modulated phases of rapid stick-slip motion per day (Bindshadler et al. 2003). During these slip events, the WIS moves forward with ice velocities that are about 40 times faster than its average flow rate, translating up to 0.4 m over a time interval of about 10 minutes (Pratt et al, 2014; Barcheck et al., 2021).

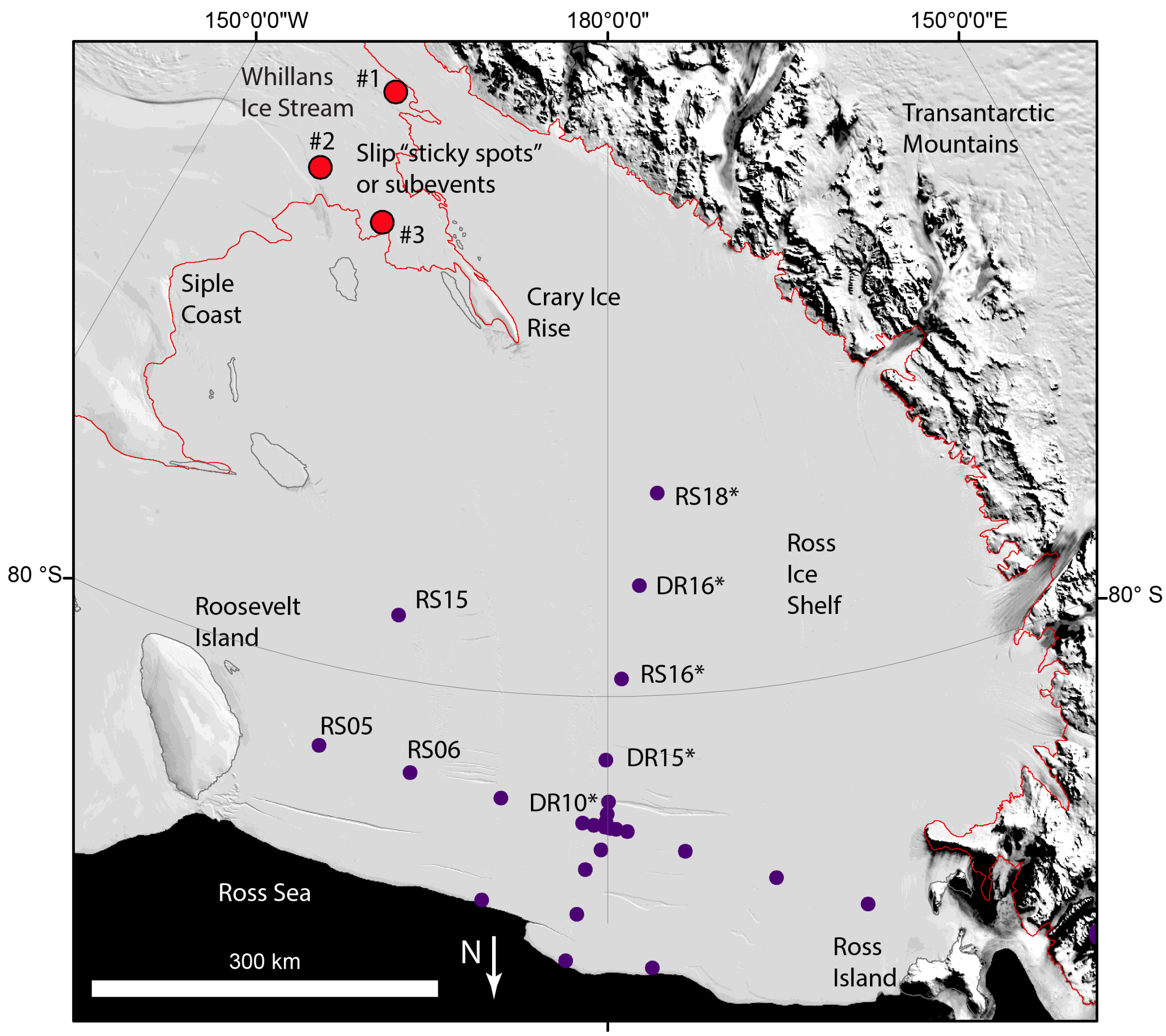

Figure 1. Geography of the Ross Ice Shelf region with seismic stations shown as blue circles. Seismic stations used in this study are labeled, with sites also equipped with GNSS receivers denoted by asterisks. The locations of Whillans Ice Stream slip asperities (Pratt et al, 2014) are shown as red circles.

As the rupture front of these basal slip events propagates across WIS, it encounters multiple regions of higher basal friction and stress, resulting in faster rupture propagation and more energetic slip (labeled as #2 and #3 on Figure 1). These "sticky spots" are similar to asperities in earthquake rupture mechanics and generate pulses of long period (15–150 s) seismic surface waves propagating in the solid earth that are observed at distances of greater than 1000 km (Wiens et al., 2008). The far-field seismic signature of these slip events is thus characterized by two or three pulses each separated by 10-15 minutes (Pratt et al, 2014). Although the rupture velocity and thus the relative pulse timing varies from event to event, and the rupture onset is not always teleseismically observable, the surface wave pulses radiate from the same regions during all events. The WIS slip events seem to be unique, likely representing a particular phase of ice stream slowdown for ice streams in the Siple Coast (Winberry et al, 2014). Although stick-slip behavior has been documented at a small scale on many glaciers (e.g., Graff and Walter, 2021), there are no other observations of such large-scale stick slip behavior involving entire glaciers or ice streams.

Until now, the effect of transient ice stream or glacier acceleration on downstream ice shelves has not been documented. In this paper, we use seismic and GNSS data from sensors deployed on the ice shelf to observe the effects of WIS slip events on the Ross Ice Shelf (RIS). We find that the WIS slip events produce elastic Lamb waves that propagate as guided waves within the RIS and are seismically observed on the shelf at distances up to 700 km. A permanent displacement pulse observed by GNSS recievers also propagates across the RIS in association with the Lamb waves, translating the entire ice shelf away from WIS. These results demonstrate that upstream disturbances in ice streams propagate across entire ice shelves, and could, in the case of large disturbances, produce strain rates that may affect ice shelf fracture and destabilization.

2 Seismic and GNSS data

The response of the RIS to WIS slip events was recorded by a network of broadband seismographs (Baker et al, 2019) and co-located GNSS receivers (Klein et al, 2020) (Figure 1) deployed on the ice shelf between 2014 and 2016. Twenty-seven broadband seismic stations were installed on the Ross Ice Shelf in late 2014 and operated continuously until late 2016 during the coordinated RIS (Mantle Structure and Dynamics of the Ross Sea from a Passive Seismic Deployment on the Ross Ice Shelf) and DRIS (Dynamic Response of the Ross Ice Shelf to Wave-Induced Vibrations) projects (Figure 1) (Baker et al., 2019; doi:10.7914/SN/XH_2014). Each station consisted of a Nanometrics 120PH posthole sensor buried to a depth of approximately 2 m below the snow surface, with data recorded at either 100 or 200 Hz by Quanterra Q330 dataloggers. The instruments were powered by solar panels during the summer and lithium batteries during the winter, so they recorded year-round. Instrument responses supplied by the Earthscope data center were deconvolved to provide three-component displacement or velocity records.

Thirteen of the RIS-DRIS stations had co-located GNSS receivers installed in November 2015, which remained in place for 1 year (Klein et al., 2020; doi:10.7283/58E3-GA46). Most of the receivers were powered by solar panels, so they did not record during the winter months. The GNSS receivers recorded at 1 Hz and were processed by Klein et al (2020) using a precise point positioning (PPP) approach (Zumberge et al., 1997) to obtain daily time series for each station. The 1 Hz time series for each station was down-sampled to 0.0333 Hz to create a time series spanning the entire observation period.

3 Extensional Lamb Waves

The RIS seismographs record clear long-period signals on the horizontal components shortly after WIS slip events. We determine the times of WIS slip events independent of any signals recorded on the ice shelf by analyzing seismic signals propagating through the solid Earth to permanently installed Global Seismographic Network seismic stations in the Dry Valleys (VNDA) and at South Pole (QSPA), with known travel times to the WIS source region (Wiens et al, 2008; Pratt et al, 2014). The signals recorded by the seismographs on the RIS consist of a series of two or three arrivals, separated by 10–15 minutes (Figure 2), with timing that is consistent with arrivals observed at the permanent off-shelf seismic stations. The signals at the RIS seismic stations, at distances of 350 – 700 km, arrive only a few seconds prior to the signals at the permanent seismic station VNDA (distance about 990 km). Previous work identified the arrivals at VNDA as primarily fundamental mode Rayleigh waves (Wiens et al, 2008; Pratt et al, 2014), with elliptical particle motion and the largest amplitude on the vertical component. However, the arrivals on the ice shelf are observed only on the horizontal components, and so must represent a different seismic phase with a velocity that is slower than the 3000-4000 m/s Rayleigh wave group velocity at 20–125 s period in this region (e.g., Shen et al., 2018).

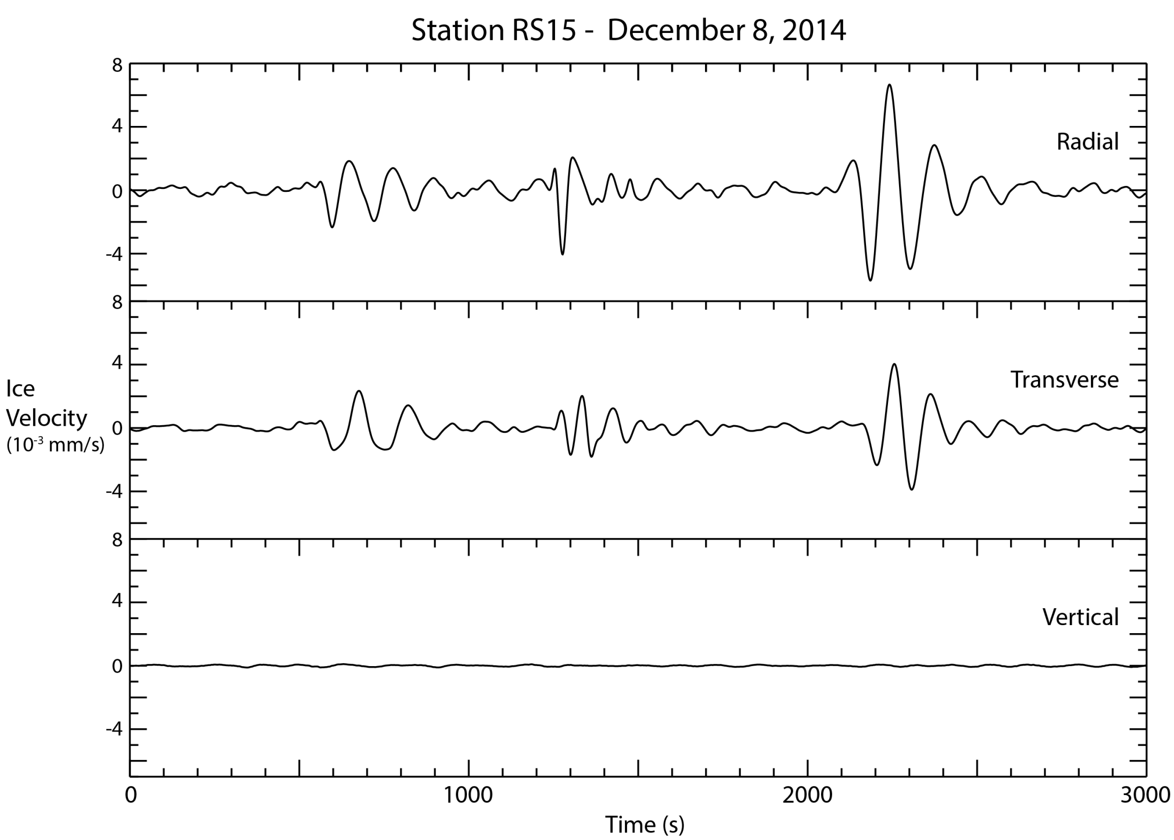

Figure 2. Broadband three-component seismic record showing extensional Lamb waves produced by the Whillans Ice Steam slip event on December 8, 2014 recorded at station RS15 (Figure 1), a distance of about 390 km. The instrument response has been deconvolved and filtered to produce velocity from 20 – 125 s.

The seismic signals show particle motions that are approximately along the great circle path connecting the station and the WIS source region, with first motions oriented radially away from WIS. Following the initial arrival, the motion of the pulses become more complex (Figure S1). The maximum signal-to-noise ratio is observed at periods between about 20 and 100 s. This is because the WIS slip events produce little short period energy and the horizontal components of seismic stations on the ice become dominated by large-amplitude ocean-propagating infragravity waves at periods longer than several hundred seconds (Bromirski et al, 2015). To estimate the phase velocity of the arrivals, we computed the power of the stacked seismograms assuming different horizontal phase velocities and a source near the WIS (Figure 3). The estimated velocity of about 2800 m/s is much slower than the P-velocity in ice (~ 3600 m/s) but much faster than the shear velocity in ice (~ 1900 m/s) or the P-velocity in water (~ 1500 m/s). We also estimated the group velocity, using approximate source times of the pulses from the Rayleigh wave arrivals at VNDA and the observed arrival times at stations on the RIS. The estimated group velocities are similar to the phase velocities, indicating there is no significant dispersion.

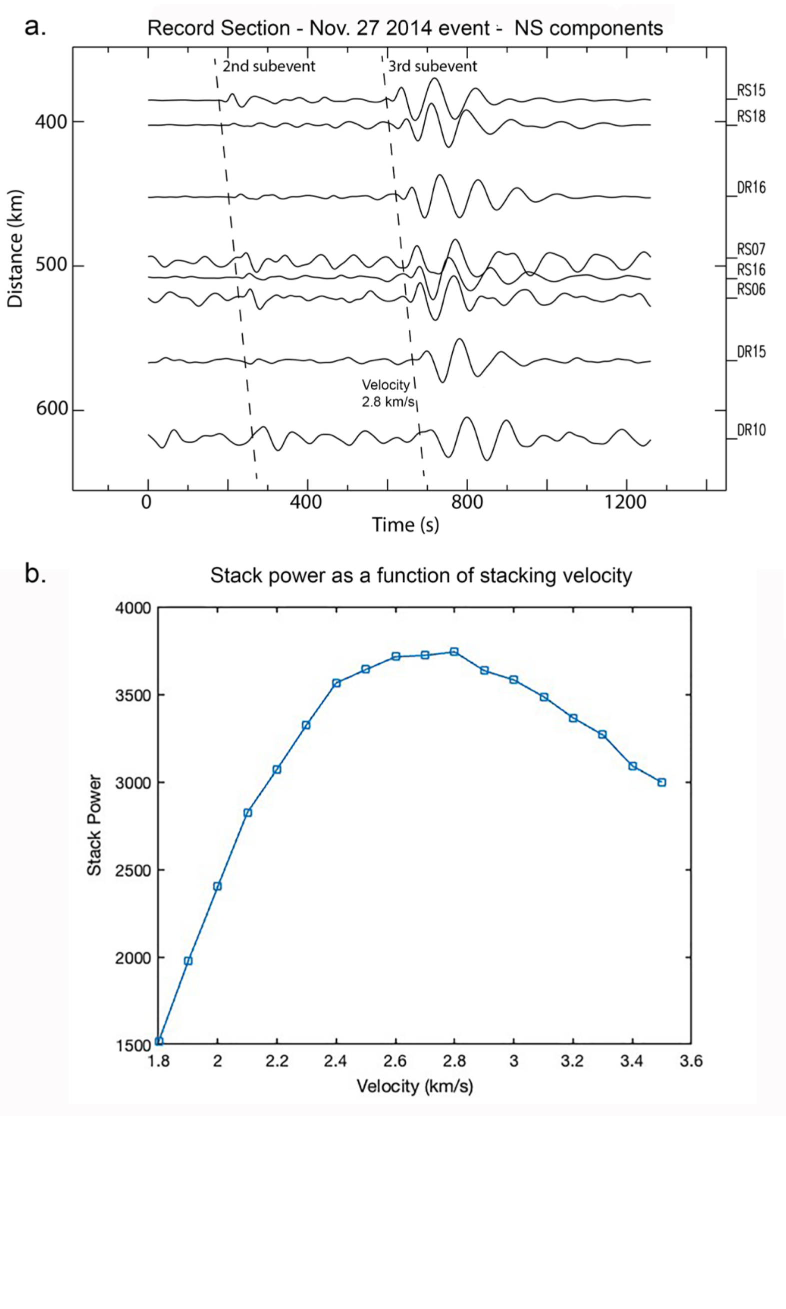

Figure 3. a) Record section from the November 27, 2014 (19:03) Whillans slip event showing the N-S component from seismographs deployed across the Ross Ice Shelf. Seismograms were filtered with a 20 – 67 s band-pass filter. The first sub-event is not visible for this event. b) Slant stack of the NS components for the November 27, 2014 event, showing the stack power as a function of stacking velocity. A velocity of 2800 m/s fits the data best and is also indicated by a dashed line in the upper figure.

We identify these arrivals as elastic plate waves, sometimes referred to as Lamb waves, propagating as guided waves in the ice shelf (Lamb, 1917). An elastic plate suspended in a vacuum gives a solution for longitudinal (extensional) waves with velocity:

$$V = 2\,V_S\,(1 - V_S^2/V_P^2)^{1/2} \qquad (1)$$

where V_S and V_P are the S and P wave velocities in the elastic plate. Press and Ewing (1951) derived a solution for an elastic plate overlying a liquid layer, arriving at the identical formula with a small imaginary term resulting in some attenuation. The equations have been rederived by many authors since that time, usually in the wavenumber domain, showing that long-period longitudinal waves in this system are a non-dispersive fundamental symmetric mode, often designated as S_0 (e.g., Graff, 1991; Chen et al., 2018). The predicted ratio of horizontal to vertical particle motion is approximately the ratio of plate thickness to the wavelength. For waves with 40 s period and the 350 m thick RIS, this ratio is greater than 300, so this solution predicts longitudinal waves with particle motion that are almost perfectly horizontal and are radial to the source, consistent with our observations. Using a Vp/Vs ratio of 1.87 corresponding to the ice Poisson's ratio of 0.3 (Squire, 2007), and Vs of 1695 m/s derived by taking the time-weighted average Vsv from the RIS seismic velocity profile of Diez et al, (2016), equation (1) predicts a velocity of 2865 m/s for the longitudinal wave speed, which is similar to the 2800 m/s that best fits the propagation across the RIS.

Longitudinal Lamb waves excited by other processes have been previously observed propagating across ice shelves via array analysis in the time, frequency, or wavenumber domain. Chen et al. (2018) and Aster et al. (2021) noted that longitudinal Lamb waves were persistently excited by swell impinging along the RIS front and used array analysis to estimate the phase velocity as 2940 m/s at 0.02 to 0.1 Hz, similar to the velocity observed in this study. Baker (2020) also noted that long-period Lamb waves observed in the RIS interior were excited at the grounded margins of the RIS by teleseismic shear waves.

4 Permanent Ice Shelf Displacement

GNSS receivers located at the seismograph sites during 2015 – 2016 record the permanent surface displacement and strain across the RIS. The GNSS signals contain low amplitude high frequency noise that precludes determination of the precise onset time of the displacement associated with the Whillans slip events, but it initiates simultaneously with or shortly after the arrival of the first large amplitude elastic plate wave and continues for 15 to 20 minutes (e.g., as shown at station RS18 in Figure 4). The total displacement is generally 50 – 60 mm and the average ice shelf velocity during the displacement episode is about 0.05 mm/s (5 m/day), compared to the approximate 2 m/day average velocity (Brunt and MacAyeal, 2014) at this station. However, the velocities are greater immediately following one of the extensional wave arrivals, reaching as high as 0.3 mm/s (26 m/day), or more than ten times the usual ice shelf velocity.

The displacement is approximately in the direction away from the WIS but varies somewhat for the different slip subevents (Figure 5). For example, at station RS18, the first subevent occurring at the southernmost sticky spot produces more northward motion on the GNSS displacement record compared to the more southerly third subevent, which produces larger westward motions (Fig 5). This is consistent with the first motions from the seismograph records, which show the same trend (Figure S1). The ice shelf displacement returns to the average flow direction within a few minutes of the final extensional wave arrival. Overall, the GNSS records indicate that the WIS slip events displace the entire RIS, with area of about 500,000 square kilometers and mass of approximately 200,000 Gigatons, by about 60 mm over a period of minutes on an almost daily basis.

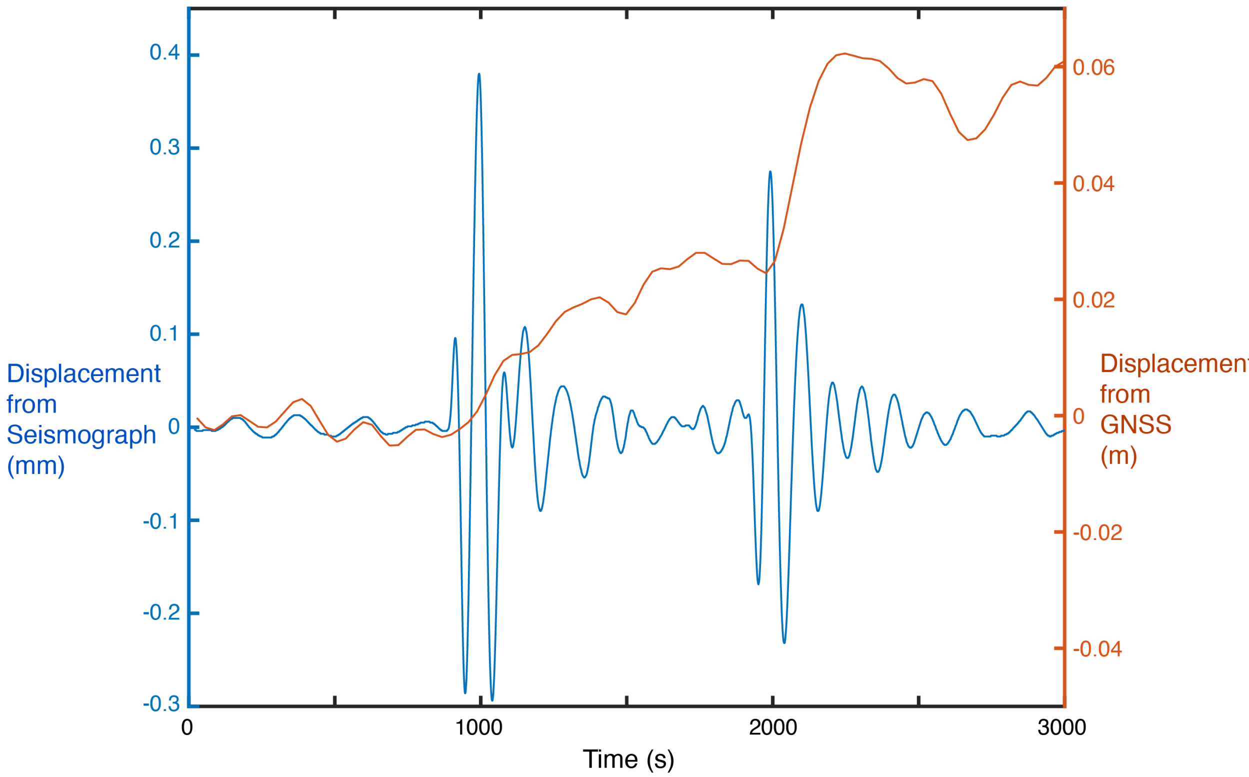

Figure 4. Comparison of displacement records of the co-located broadband seismograph and GNSS receiver at station RS18 for the Whillans slip event of December 7, 2015 (16:19). Both records have been rotated into the back-azimuth of the WIS to give radial displacement records. Seismic data are filtered with a causal bandpass filter between 0.05 and 0.008 Hz to remove noise. GNSS data have been detrended to remove the long-term ice flow and filtered with a causal low pass filter at 0.005 Hz. Signals from the first and third subevents are visible on both records; the second subevent is absent at this station due to obstruction by the northernmost extent of WIS and Crary Ice Rise.

Ideally, it would be useful to sample the displacement field continuously across the seismic spectrum to determine more precisely the relationship between the higher frequency elastic wave arrivals and the permanent displacement pulse. However, the seismic sensors (Trillium 120 posthole) have reduced sensitivity beyond the 120 s corner period and horizontal component signals become dominated by ocean infragravity waves at periods greater than about 150 s. The displacements recorded by RIS GNSS receivers also have high noise at these periods consistent with the infragravity wave background displacement field, which has rms amplitudes of several cm (Bromirski et al, 2015; 2017). Thus, we interpret the seismic and GNSS signals separately in high signal-to-noise and relatively band-limited windows of about 20–125 s for the seismic data showing the elastic wave propagation, and at very long periods near zero frequency for the GNSS data constraining the permanent ice shelf displacement.

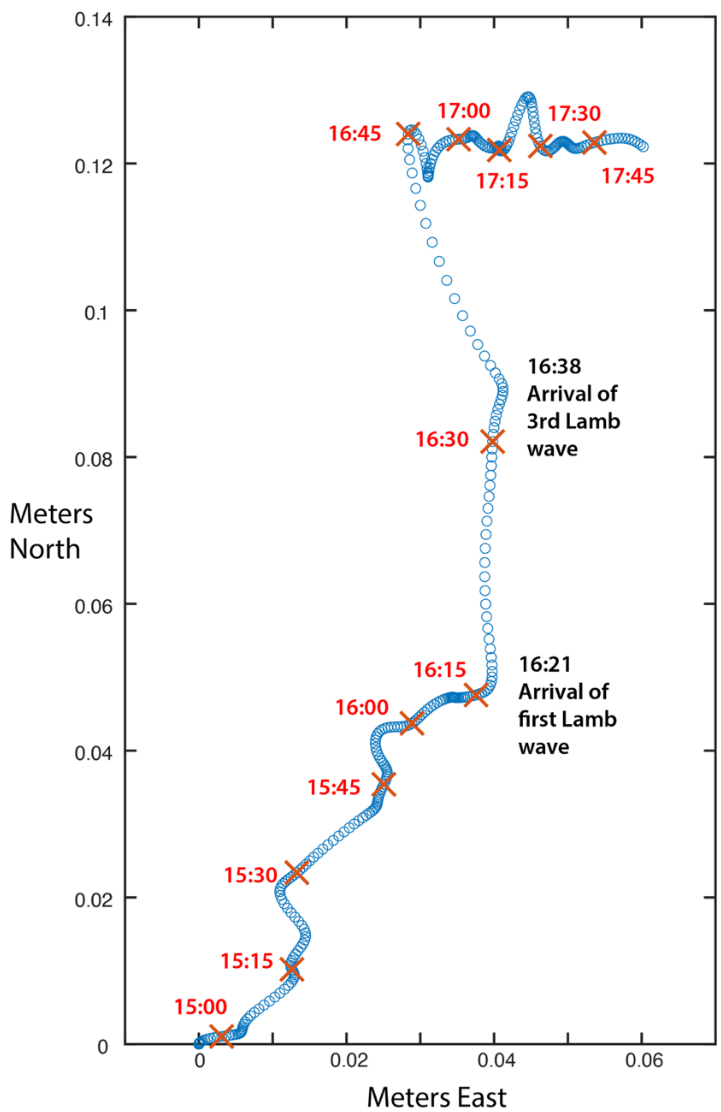

Figure 5. Map view of the displacement trajectory of station RS18 (Figure 1) during December 7, 2015, determined by GNSS, showing the changes in speed and direction caused by Whillans slip events. The displacements have been smoothed using a 900 s causal low-pass filter. Open circles denote positions every 30 s. 15-minute time stamps are shown as red x's. The average annual flow velocity determined by Klein et al (2020) has been subtracted from the motion, but some background motion remains due to seasonal and tidal fluctuations.

5 Discussion and Conclusions

These results demonstrate that large-scale stick-slip motion of an ice stream can transmit elastic waves and strain pulses across its downstream ice shelf, modifying and briefly dominating the motion of an entire ice shelf with lateral dimensions of nearly 1000 km. Ice streams and their associated ice shelves thus constitute a single elasto-dynamical system, with persistent ice stream events possibly influencing ice shelf stability and deformation. The large number of recorded ice stream signals in this data set also show that ice shelf stick-slip events can be easily monitored and assessed using instrumentation placed on the ice shelf hundreds of kilometers away.

A particularly interesting implication is that dynamic strain from the extensional waves or the permanent strain pulse could trigger icequakes, thus facilitating deformation and fracture of the ice shelf. We estimate the peak dynamic strain experienced by the ice shelves during passage of the extensional waves and the displacement pulse using the relationship:

$$|\varepsilon_{rr}| \sim (1/V)\, \partial U_r/\partial t \qquad (2)$$

Where V is the phase velocity of the propagating wave and U_r is the radial particle displacement (Gomberg and Agnew, 1996). The stress is given by:

$$\sigma_{rr} = E\, \varepsilon_{rr} /(1-\nu) \qquad (3)$$

Where E is Young's modulus and ν is Poisson's ratio (approximately 10 GPa and 0.3, respectively, for ice). The largest WIS-associated ice velocities recorded at the GNSS receivers are about 0.3 mm/s, with the largest particle velocities inferred from the band-limited seismographs being somewhat smaller. Using the phase velocity of 2800 m/s from the previous section gives a peak dynamic strain of about 10^{-7} and a radial normal stress of 1.4 KPa.

These dynamic strains and stresses are similar to those observed to trigger seismicity during the passage of seismic surface waves from giant earthquakes worldwide. Peak dynamic strains on the order of 10^{-7} triggered earthquakes in Alaska following the 2012 Sumatra earthquake (Tape et al, 2013), and Fan et al. (2021) observe some triggering in California for many teleseisms with peak dynamic strains as low as 10^{-9}. Icequakes are also triggered by teleseismic surface waves in the Antarctic ice sheet and on mountain glaciers with peak dynamic strains as small as 10^{-8} (Peng et al, 2014; Li et al, 2021).

These observations suggest that extensional waves and strain pulses from WIS stick-slip events could mobilize fractures in the ice shelf interior and contribute to its destabilization. However, up to now there are no documented cases of icequakes in the ice shelf that are clearly triggered by WIS slip events. Olinger et al (2019) located more than 2,500 icequakes along rift WR4 near the intersection of the two lines of RIS seismic stations (Figure 1) but did not detect any greater seismicity during the passage of waves from Whillans slip events. This may be due to the fact that rift WR4 is deforming in tension, with icequakes likely confined to the upper few meters of snow and ductile deformation at deeper levels (Huang et al, 2022), whereas the strain pulses from the WIS slip events exert dominantly compressional stress across the entire thickness of the shelf.

The WIS is the only location worldwide where such large-scale stick-slip events have been documented and it is unclear how typical the current activity is over longer time intervals. The WIS flow rate has been decreasing, likely due to increased friction due to decreased subglacial meltwater (Stearns et al, 2005). This velocity decrease has resulted in fewer slip events, with some of the normal twice-daily slip events being skipped and larger slip then occurring during the next slip event (Winberry et al, 2014). If the dynamics of the slowing ice stream reach a point where larger slip events occur, it is possible that the extensional waves and strain pulse from larger slip events could have a greater effect on the deformation and stability of the RIS.

Acknowledgments

This research was supported by NSF grants PLR-1142518, 1141916, 1142126, 1246151, 1246416, OPP1744856, and OPP-1744889. The facilities of EarthScope Consortium were used for access to waveforms and related metadata. These services are funded through the Seismological Facility for the Advancement of Geoscience (SAGE) Award of the U.S. National Science Foundation (NSF) under Cooperative Support Agreement EAR-1851048 and Geodetic Facility for the Advancement of Geoscience (GAGE) Award under NSF Cooperative Agreement EAR-1724794. The Global Seismographic Network (GSN) is a cooperative scientific facility operated jointly by NSF and the United States Geological Survey (USGS). The NSF component is part of the SAGE Facility, operated by EarthScope Consortium under Cooperative Support Agreement EAR-1851048.

Open Research

Seismic data used in this study are available through the Earthscope Data Management Center under Ross Ice Shelf (RIS) and DRIS network code XH: https://www.fdsn.org/networks/detail/XH_2014/. Raw GNSS data are archived by the EarthScope Data Management Center: https://doi.org/10.7283/58E3-GA46. Final GNSS processed data are archived by the Scripps Orbit and Permanent Array Center: http://garner.ucsd.edu/pub/projects/RossIceShelfAntarctica/

References

Anandakrishnan S., Voigt D. E, Alley R. B. and King M. A. (2003), Ice Stream D flow speed is strongly modulated by the tide beneath the Ross Ice Shelf. *Geophysical Research Letters*, **30**(7), 1361, doi: 10.1029/2002GL016329

Aster, R. C., Lipovsky, B. P., Cole, H. M., Bromirski, P. D., Gerstoft, P., Nyblade, A., et al., (2021). Swell-Triggered Seismicity at the Near-Front Damage Zone of the Ross Ice Shelf. *Seismological Research Letters,* doi:10.1785/0220200478

Baker, M. G., Aster, R. C., Anthony R. E., Chaput, J., Wiens, D. A., Nyblade, A., et al, (2019). Seasonal and spatial variations in the ocean-coupled ambient wavefield of the Ross Ice Shelf. *Journal of Glaciology*, 1-14, doi.org/10.1.017/jog.2019.64

Baker, M. G., Aster, R. C., Wiens, D. A., Nyblade, A. A., Bromirski, P. D., Gerstoft, P. et al., (2020) Teleseismic earthquake wavefields observed on the Ross Ice Shelf, *Journal of Glaciology*, 1-17, doi: 10.1017/jog.2020.83

Barcheck, G., E. E. Brodsky, P. M. Fulton, M. A. King, M. R. Siegfried and S. Tulaczyk (2021). Migratory earthquake precursors are dominant on an ice stream fault**,** *Science Advances,* **7** (6), eabd0105. doi: 10.1126/sciadv.abd0105.

Berthier, E., Scambos, T.A., and Shuman, C.A. (2012). Mass loss of Larsen B tributary glaciers (Antarctic Peninsula) unabated since 2002. *Geophysical Research Letters*, 39 (13), L13501. doi: 10.1029/2012gl051755.

Bindschadler RA, King, M.A., Alley, R.B., Anandakrishnan, S. and Padman, L. (2003) Tidally controlled stick–slip discharge of a West Antarctic ice stream. *Science*, **301**(5636), 1087–1089, doi: 10.1126/science.1087231

Bromirski, P. D., Diez, A., Gerstoft, P., Stephen, R. A., Bolmer, T., Wiens, D. A., et al., (2015), Ross ice shelf vibrations, *Geophysical Research Letters*, 42, 7589–7597, doi:10.1002/ 2015GL065284.

Bromirski, P.D., Chen, Z., Stephen, R. A., Gerstoft, P., Arcas, D., Diez, A., et al, (2017). Tsunami and infragravity waves impacting Antarctic ice shelves, *Journal of Geophysical Research-Oceans*, **122**, doi:10.1002/2017JC012913.

Brunt K. M., King, M. A., Fricker, H.A. and MacAyeal D.R. (2010) Flow of the Ross Ice Shelf, Antarctica, is modulated by the ocean tide. *Journal of Glaciology*, **56**(195), 157–161, doi: 10.3189/ 002214310791190875

Brunt, K. M., and MacAyeal, D. R. (2014) Tidal modulation of ice-shelf flow: a viscous model of the Ross Ice Shelf, *Journal of Glaciology*, 60, 500-508, doi: 10.3189/2014JoG13J20.

Chen, Z., Bromirski, P. D., Gerstoft, P., Stephen, R. A., Wiens, D. A., Aster, R. C., and Nyblade, A. A., (2018) Ocean-excited plate waves in the Ross and Pine Island Glacier ice shelves, *Journal of Glaciology,* doi: 10.1017/jog.2018.66

Diez, A., Bromirski, P. D., Gerstoft, P., Stephen, R. A., Anthony, R. E., Aster, R. C., et al, (2016) Ice shelf structure derived from dispersion curve analysis of ambient seismic noise, Ross Ice Shelf, Antarctica, *Geophysical Journal International, 205*, 785-795, doi:10.1093/gji/ggw036

Dupont, T. K., and Alley, R. B. (2005), Assessment of the importance of ice-shelf buttressing to ice-sheet flow, *Geophysical Research Letters, 32*, L04503, doi:10.1029/2004GL022024.

Fan, W., Barbour, A. J., Cochran, E. S., & Lin, G. (2021). Characteristics of frequent dynamic triggeringof microearthquakes in Southern California. *Journal of Geophysical Research: Solid Earth*, *126*, e2020JB020820. https://doi. org/10.1029/2020JB020820

Goldberg, D., Holland, D. M., and Schoof, C. (2009), Grounding line movement and ice shelf buttressing in marine ice sheets, *Journal of Geophysical Research*, 114, F04026, doi:10.1029/2008JF001227.

Gomberg, J., Agnew, D. (1996), The accuracy of seismic estimates of dynamic strains: An evaluation using strainmeter and seismometer data from Pinion Flat Observatory, California, *Bulletin of the Seismological Society of America*, 86, 212-220.

Graff, K. F. (1991) *Wave Motion in Elastic Solids*, Revised Edn. Dover Publications, New York. 688 pp.

Graff, D., and Walter, F. (2021), Changing friction at the base of an alpine glacier, *Scientific Reports*, 11:10872, doi.org/10.1038/s41598-021-90176-9

Huang, M.-H., Udell Lopez, K., & Olsen, K. G. (2022). Icequake-magnitude scaling relationship along a rift within the Ross Ice Shelf, Antarctica. *Geophysical Research Letters*, *49*, e2022GL097961. https://doi.org/10.1029/2022GL097961

King, M., A., Makinson, K., and Gudmundsson, G. H. (2011) Nonlinear interaction between ocean tides and the Larsen C Ice Shelf system. *Geophysical Research Letters*, **38**(8), L08501, doi: 10.1029/ 2011GL046680

Klein, E., Mosbeux, C., Bromirski, P.D., Padman, L., Bock, Y., Springer, S.R., Fricker, H.A. (2020). Annual cycle in flow of Ross Ice Shelf, Antarctica: contribution of variable basal melting. *Journal of Glaciology*, 1–15. doi.org/10.1017/jog.2020.61

Lamb, H. (1917), On elastic waves in a plate, *Proceedings of the Royal Society London, A93*, 114.

Li, C., Peng, Z., Chaput, J. A., Walter, J. I., and Aster, R. C. (2021). Remote Triggering of Icequakes at Mt. Erebus, Antarctica by Large Teleseismic Earthquakes, *Seismological Research Letters*, 1–10, doi: 10.1785/ 0220210027.

Martin, D. F., Cornford, S. L., & Payne, A. J. (2019). Millennial-scale vulnerability of the Antarctic Ice Sheet to regional ice shelf collapse. *Geophysical Research Letters, 46,* 1467–1475. https://doi.org/10.1029/2018GL081

Olinger, S., Lipovsky, B. P., Wiens, D. A., Aster, R. C., Bromirski, P. D., Chen, Z., et al. (2019). Tidal and thermal stresses drive seismicity along a major Ross Ice Shelf rift. *Geophysical Research Letters*, *46*. https://doi.org/10. 1029/2019GL082842

Peng, Z., Walter, J. I., Aster, R. C., Nyblade, A., Wiens, D. A., and Anandakrishnan, S., (2014) Antarctic icequakes triggered by the 2010 Maule earthquake in Chile, *Nature Geoscience, 7*, 677–681.

Pratt, M. J., Winberry, J. P., D. A. Wiens, S. Anandakrishnan, and R. B. Alley (2014), Seismic and geodetic evidence for grounding-line control of Whillans Ice Stream stick-slip events, *Journal of Geophysical Research: Earth Surface*, *119,* 333–348, doi:10.1002/ 2013JF002842.

Press, F., and Ewing, M. (1951), Propagation of elastic waves in a floating ice sheet, *EOS Transactions American Geophysical Union, 32*, 673-678.

Scambos, T. A., Bohlander, J. A., Shuman, C. A., and Skvarca, P. (2004), Glacier acceleration and thinning after ice shelf collapse in the Larsen B embayment, Antarctica, *Geophysical Research Letters, 31*, L18402, doi:10.1029/2004GL020670.

Shen, W., Wiens, D. A., Anandakrishnan, S., Aster, R. C., Gerstoft, P., Bromirski, P. D., et al. (2018) The crust and upper mantle structure of central and West Antarctica from Bayesian inversion of Rayleigh wave and receiver functions. *Journal of Geophysical Research: Solid Earth, 123,* 7824–7849, doi:10.1029/ 2017JB015346.

Squire, V. A. (2007) Ocean waves and sea-ice revisited, *Cold Regions Science and Technology*, *49,* 110-133.

Stearns, L. A., Jezek, K. C., and van der Veen, C. J. (2005), Decadal-scale variations in ice flow along Whillans Ice Stream and its tributaries, West Antarctica, *Journal of Glaciology, 51,* 147-157.

Tape, C., West, M., Silwal, V., Ruppert, N. (2013) Earthquake nucleation and triggering on an optimally oriented fault, *Earth and Planetary Science Letters, 363*, 231-241, doi:10.1016/j.epsl.2012.11.060

Wiens, D. A., Anandakrishnan, S., Winberry, J. P., and King, M. A., (2008) Simultaneous teleseismic and geodetic observations of the stick-slip motion of an Antarctic ice stream, *Nature, 453*, 770-774

Winberry, J. P., Anandakrishnan, S., Alley, R. B., Wiens, D. A., and Pratt, M. J. (2014), Tidal pacing, skipped slips, and the slowdown of Whillans Ice Stream, Antarctica, *Journal of Glaciology, 60*, 222, doi: 10.3189/2014JoG14J038

Zumberge J., Heflin M., Jefferson D., Watkins M. and Webb F.H. (1997) Precise point positioning for the efficient and robust analysis of GPS data from large networks. *Geophysical Research Letters 33,* L23312. doi: 10.1029/96JB03860.